The N-Terminus of Retinol Dehydrogenase Type 1 Signals Cytosolic Orientation in the Microsomal Membrane†

Jin Wang, Juliet K. Bongianni, and Joseph L. Napoli*

Department of Nutritional Sciences and Toxicology, University of California, Berkeley, California 97420-3104

Received July 5, 2001; Revised Manuscript Received August 15, 2001

ABSTRACT: We determined the orientation of the SDR (short-chain dehydrogenase/reductase) rat RoDH1 (retinol dehydrogenase type 1) in the endoplasmic reticulum to provide insight into its function in retinol metabolism, and to resolve whether retinoid-metabolizing SDRs differ from several other SDRs by requiring a C-terminal segment for the membrane orientation. In contrast to several soluble SDRs, the membrane-associated RoDH1 has hydrophobic extensions N- and C-terminal to the SDR core. Confocal microscopy and/or proteinase K protection assays of RoDH1, RoDH1 mutants, and RoDH1−green fluorescent protein fusion proteins showed that the N-terminal segment anchors RoDH1 to the endoplasmic reticulum membrane facing the cytosol. The C-terminal hydrophobic segment increases the relative proportion of RoDH1 associated with the endoplasmic reticulum, but has no affect on orientation. Deletion of either or both extensions causes nearly total loss of enzyme activity, possibly through altering the nature of RoDH1 association with membranes, or destabilizing the enzyme, but does not alter the expression of RoDH1 or convert it into a soluble protein. The latter suggests that the SDR core of RoDH1 has marked external hydrophobicity that causes nonspecific membrane association.

atRA[1] functions as a hormone in vivo that regulates numerous biological processes by controlling gene transcription (*1*, *2*). Three nuclear hormone receptors (RARα, -*β*, and -*γ*) mediate atRA-induced transcriptional activation during multiple phases of development, and continue to act throughout the lives of all vertebrates (*3*, *4*). Two-step metabolism of retinol (vitamin A), a molecule without biological activity per se, generates the endocrine factor atRA (*5*). The first and rate-limiting step of atRA biosynthesis from retinol relies on reversible dehydrogenation into retinal. Dehydrogenation of retinal produces atRA irreversibly, and may serve as a rate-determining event. Members of two classes of enzymes (the medium-chain alcohol dehydrogenases, ADHs, and the SDRs) convert all-*trans*-retinol into all-*trans*-retinal in vitro (*5*, *6*). Only certain members of the SDR family, e.g., rat RoDH1 and human RoDH-E, recognize the major physiological form of retinol, retinol bound with the cytosol protein CRBP (*7*−*10*). Of these, rat liver microsomal RoDH has lower apparent K_m values with holo-CRBP versus unbound retinol, and catalyzes retinal synthesis in the presence of excess apo-CRBP. Because the CRBP−retinol interaction has an apparent K_d of <0.1 nM (*11*), synthesis of atRA in the presence of total CRBP exceeding total retinol, with the concentrations of both in the micromolar range, must be driven by enzyme access to CRBP-bound retinol. Although dehydrogenases that recognize holo-CRBP occur in cytosol, they are inhibited severely by a small excess of apo-CRBP. Even uninhibited, they provide a much smaller contribution to the total retinal-generating enzyme units than microsomal RoDH (*8*, *9*).

The first 18 amino acid residues of the rat microsomal SDR RoDH1 form a hydrophobic helix consistent with a membrane directing and/or anchoring function, but this segment does not undergo cleavage (*12*). A cleavable hydrophobic signal peptide at the N-terminus targets proteins for the lumen of the ER, whereas signal peptides that do not undergo cleavage indicate membrane-anchored proteins that can face either the lumen or the cytosolic sides of the ER (*13*). For some integral membrane proteins, a distinct C-terminal transmembrane domain acts as a membrane anchor. Enzymes resident as soluble lumen proteins usually undergo glycosylation, and contain a consensus motif, KDEL, usually located at the C-terminus (*14*, *15*). RoDH1 contains no KDEL motif and does not appear to be glycosylated, because it migrates on SDS−PAGE according to the molecular mass deduced from its cDNA (*8*, *12*).

Different models have been proposed to describe the interaction of SDR with membranes (*16*−*18*). h11*β*HSD1, for example, uses a single N-terminal hydrophobic segment as a membrane anchor, with the bulk of the enzyme projecting into the lumen of the ER (*16*). h11*β*HSD2 has the opposite topology; it anchors to the ER projecting into the cytosol (*18*). The N-terminal transmembrane segments seem sufficient to lead h11*β*HSD1 and -2 to the ER, and to determine their orientation (*18*, *19*). In contrast, the 11-*cis*-RoDH orthologs (mouse RDH4 and human RDH5)

† This work was supported by NIH Grant DK36870.

* To whom correspondence should be addressed: Department of Nutritional Sciences and Toxicology, 119 Morgan Hall, MC#3104, University of California, Berkeley, CA 97420-3104. Phone: (510) 642-0908. Fax: (510) 642-0535. E-mail: jna@uclink4.berkeley.edu.

[1] Abbreviations: atRA, all-*trans*-retinoic acid; ConA, concanavalin A; CRAD, *cis*-retinol/androgen dehydrogenase; CRBP, cellular retinol-binding protein type I; ER, endoplasmic reticulum; GFP, green fluorescent protein; h11*β*HSD1 or -2, 11*β*-hydroxysteroid dehydrogenase type 1 or 2, respectively; PBS, phosphate-buffered saline; RoDH, retinol dehydrogenase; SDR, short-chain dehydrogenase/reductase.

10.1021/bi011396+ CCC: $20.00
Published on Web 09/28/2001

reportedly rely on N- and C-terminal hydrophobic segments as ER membrane anchors, with the bulk of the proteins projecting into the lumen (*17*, *20*). Unfortunately, no common structural motifs have emerged that indicate how other membrane-bound SDRs anchor to the ER, and whether they face the lumen or the cytosol.

This study had two purposes: to provide additional insight into the precise function of RoDH1 in retinol metabolism by determining its ER orientation and to determine whether retinoid-metabolizing SDRs differ from steroid-metabolizing SDRs by requiring a C-terminal segment for ER association and/or orientation. The data show that RoDH1 requires both N- and C-terminal hydrophobic segments for appreciable activity. The RoDH1 N-terminal hydrophobic segment serves as a necessary and sufficient signal that directs the enzyme to the ER and anchors it facing the cytosol. The C-terminal hydrophobic segment enhances ER association, but does not direct the orientation of RoDH1. Thus, RoDH1 is an ER-anchored, cytosol-facing SDR.

EXPERIMENTAL PROCEDURES

Expression Vectors. pcDNA3/RoDH1 was constructed by inserting the coding region of rat RoDH1 into the mammalian expression vector pcDNA3 between the *Bam*HI and *Eco*RI sites. cDNAs encoding truncated mutants of RoDH1 were amplified by PCR. RoDH1(Δ1−18) relied on the primers 5′-CATGGATCCACCATGAGGGAGAGGAAGGTG (sense) and 5′-CATGGAATTCCCCAAGTCTGCACACAT (antisense). RoDH1(Δ289−317) used the primers 5′-GATCGGATCCACCATGTGGCTCTACCTG (sense) and 5′-GATCGAATTCTCACTTGGCATCC (antisense). RoDH1(Δ1−18+Δ289−317) was amplified with the primers 5′-CATGGATCCACCATGAGGGAGAGGAAGGTG (sense) and 5′-GATCGAATTCTCACTTGGCATCC (antisense). PCR products were digested with *Bam*HI and *Eco*RI and subcloned into pcDNA3. For RoDH1(Δ289−311), a cDNA encoding amino acids 1−288 was amplified with primers 5′-GATCGGATCCACCATGTGGCTCTACCTG (sense) and 5′-CTTGGCATCCCAACCA (antisense), and a cDNA encoding amino acids 312−317 was amplified with primers 5′-AAGCCTGCCCGAGCC (sense) and 5′-CATGGAATTCCCCAAGTCTGCACACAT (antisense). The PCR products were treated with *Bam*HI and *Eco*RI, respectively, and were ligated and subcloned into pcDNA3 in one reaction. The Kozak sequence was introduced before the ATG codon in all mutants.

The RoDH1(1−22)−GFP fusion protein was constructed by inserting the first 22 N-terminal amino acid residues of RoDH1 immediately before the coding region of GFP in pEGFP-N1 (*19*). First, a cDNA encoding residues 1−22 of RoDH1 (by the Kozak sequence), with an *Eco*RI site at the 5′-end, and extended by a *Bcl*I site at the 3′-end, was amplified by PCR using primers 5′-CTTGGAATTCCCACCATGTGGCTCTACCTGCT (sense) and 5′-TGGATTGATCACCCTCTCCCTCAAGAAGCG (antisense). Second, the coding sequence of GFP was amplified from pEGFP-N1 by PCR using a 5′-oligonucleotide that contained a *Bcl*I site (5′-ATGGTGATCAAGGGCGAGGAG) and 3′-oligonucleotide containing a *Not*I site (5′-CCTCTACAAATGTGGTATGGC). This was done to remove the Kozak sequence preceding the first ATG codon of GFP in the pEGFP-N1 vector so that the initiation codon introduced in the N-tag sequence would be used. The PCR products were purified and digested with *Eco*RI−*Bcl*I and *Bcl*I−*Not*I fragments for N-tags and GFP, respectively, and inserted into *Eco*RI−*Not*I-digested pEGFP-N1 in a one-step ligation. Other GFP chimeras were constructed similarly. For the RoDH1−GFP fusion protein, a cDNA encoding the entire RoDH1 was amplified with primers 5′-CTTCGAATTCCCACCATGTGGCTCTACCTGCT (sense) and 5′-TGGATTGATCAACAGGGCTCGGGC (antisense). An h11βHSD1(1−41)−GFP expression vector was made by PCR amplifying an h11βHSD1 cDNA from human kidney cDNA with primers 5′-GAGGATCCGCCATGGCTTTTATGA (sense) and 5′-GATCTAGATCCTACTTGTTTAT (antisense). A cDNA of the 41 N-terminal amino acids of h11βHSD1 was amplified from the first PCR product by PCR with the same sense primer and an antisense primer extended with a *Bcl*I site (5′-TGGATTGATCAATTCCTCGTTTGCAGA). The PCR product and the *Bcl*I−*Not*I-treated GFP fragment was inserted into the *Bam*HI−*Not*I-digested pEGFP-N1 vector in a one-step ligation.

To make a construct encoding the RoDH1(1−22)−GFP−RoDH1(Δ289−317) fusion protein, a cDNA encoding the RoDH1(1−22)−GFP protein was amplified with the sense primer 5′-CTTGGAATTCCCACCATGTGGCTCTACCTGCT and the antisense primer 5′-GATCAAGCTTGTACAGCTCGTC. A cDNA fragment encoding RoDH1(Δ289−317) was amplified with the sense primer 5′-GATCAAGCTTTTCTTCTACCTCCCC and the antisense primer 5′-CATGGAATTCCCCAAGTCTGCACACAT. The PCR products were digested with *Eco*RI and *Hin*dIII. The RoDH1-(1−22)−GFP protein and RoDH1(Δ289−317) were ligated into *Eco*RI-digested pcDNA3 in one step to make the RoDH1(1−22)−GFP−RoDH1(Δ289−317) fusion protein. All constructs were sequenced.

Antibody Generation and Purification. The peptide NH_2-NLKKLWDQTTEEVK-COOH corresponding to residues 222−235 of rat RoDH1 was used to raise rabbit antisera (Bio-Synthesis, Inc.). Antiserum (5 mL) was diluted 1:1 in PBS and passed three times through a column made by coupling the peptide (1 mg) to 1 mL of NHS-activated Sepharose 4 Fast Flow gel (Amersham Pharmacia Biotech). The column was washed with 15 mL of PBS and eluted with 0.1 M glycine (pH 2.2) in 0.5 mL fractions directly into 0.1 mL of 1 M Tris-HCl (pH 8.0). Protein-containing fractions were pooled and stored in 50% glycerol at ∼0.2 mg/mL.

Immunofluorescence Assay. CHO-K1 cells were grown to 80% confluence in F-12 medium with 10% fetal bovine serum on glass cover slips placed in 60 mm plates. The cells were transfected with 1 μg of expression vectors mixed with 15 μL of LipofectAMINE reagent. Immunostaining was done 48 h post-transfection. Cells were fixed for 15 min at 25 °C using 2% paraformaldehyde in PBS and were washed three times with PBS, and incubated for 20 min at 25 °C with PBS containing 1% BSA and 0.5% Triton X-100. The glass cover slips were blocked with 10% goat serum in 1× PBS for 1 h and incubated with anti-RoDH1 (1:100) for 1 h at 25 °C. The cover slips were washed three times with PBS and incubated with fluorescein-conjugated secondary antibody (Molecular Probes). The cover slips then were incubated for 45 min at 25 °C with 0.1 mg/mL ConA in PBS containing 1% BSA, washed three times with PBS, and

mounted using Fluoromount-G (Electron Microscopy Sciences). Analyses were done with a LSM510 confocal microscope (Carl Zeiss) at 630-fold magnification.

Rat Liver Microsomes. Rat liver was homogenized in 10 mM Hepes, 250 mM sucrose, and 1 mM EDTA (pH 7.5) (homogenization buffer) by 15−20 strokes in a glass Dounce homogenizer at 4 °C. Cell debris and nuclei were pelleted at 1000*g* for 30 min. The supernatant was centrifuged at 25000*g* for 30 min. The resulting supernatant was centrifuged at 34000*g* for 45 min. This supernatant was centrifuged at 100000*g* for 1 h. The pellet (microsomal fraction) was resuspended in homogenization buffer and stored at −70 °C in aliquots.

Transient Transfection of CHO Cells and Subcellular Fractionation. CHO-K1 cells were cultured in 100 mm tissue culture dishes and transfected as described previously (*21*). Cells were harvested 24 h post-transfection. Cell pellets were suspended in homogenization buffer, disrupted by sonication on ice, and centrifuged at 1000*g* for 10 min. The supernatant was centrifuged at 10000*g* for 30 min. This supernatant was centrifuged at 100000*g* for 1 h at 4 °C. The last pellet (microsomal membrane fraction) was resuspended in homogenization buffer.

Glycerol Extraction of Microsomes and Proteinase K Protection Assay. To remove peripheral membrane proteins, microsomal membranes were resuspended in a buffer of 20 mM KH_2PO_4 (pH 8.0) and 20% glycerol and incubated at 4 °C for 30 min. The mixture was centrifuged at 100000*g* for 1 h, and the pellet was resuspended in homogenization buffer. The glycerol-extracted microsomes were diluted in PBS. Proteinase K was added to a final concentration of 50 μg/mL, and the reaction was allowed to run for 2 h in the presence or absence of 1% Triton X-100. Samples were quenched on ice for 10 min with 2 mM phenylmethanesulfonyl fluoride and were analyzed by Western blotting.

Endoglycosidase H Treatment. Microsomes were solubilized at room temperature in 0.1% SDS and 100 mM 2-mecaptoethanol and heated at 100 °C for 2 min. The solubilized proteins were incubated at 37 °C for 12 h with or without endoglycosidase H (1 milliunit/μL) in 50 mM sodium citrate (50 μL, pH 5.5).

Enzyme Activity. RoDH assays were done at 37 °C in 0.25 mL of a mixture of 50 mM Hepes, 150 mM KCl, 1 mM EDTA, and 2 mM NAD^+ (pH 8) with the 1000*g* supernatant of transfected CHO cell lysates. The reactions were quenched with 0.1 mL of 0.1 M *O*-ethylhydroxylamine and 0.35 mL of methanol, and the mixtures were incubated at room temperature for 30 min and extracted with two 2.5 mL portions of hexane. The retinoids in the hexane extract were quantified by normal-phase high-performance liquid chromatography with a detection limit of <1 pmol as described previously (*22*).

Western Blotting. Proteins were separated by 12.5% SDS−PAGE and were electrotransferred onto nitrocellulose membranes (Sigma). Membranes were blocked with 5% dry milk in PBS with 0.05% Tween 20 (PBST). After three washes with PBST, membranes were incubated for 1 h at room temperature with anti-RoDH1 (1:2000 dilution) or with mouse monoclonal anti-GFP antibody (Clontech) at 1:1000 dilution. Membranes were washed with PBST and incubated with horseradish peroxidase-labeled goat anti-rabbit IgG (1:10000) or rabbit anti-mouse IgG (1:10000) (Sigma). Signals were visualized with a chemiluminescence reagent kit (NEN). In some experiments, signals were quantified with a Chem-Imager system (Alpha Innotech Corp.).

RESULTS

Analysis of RoDH1 Structure. Soluble SDRs generally consist of 250−280 amino acid residues (*23*, *24*). Alignment of RoDH1 with several soluble SDRs reveals that RoDH1 extends at both the N- and C-terminal ends, and that the extension contains potential transmembrane regions (Figure 1). The first 18 N-terminal residues of RoDH1 form a helix, sufficiently long and hydrophobic for membrane anchoring (*12*). A short stretch of hydrophilic residues, $R^{19}ERK$, flanks this hydrophobic span, a feature typical at membrane junctures, presumably to position the enzyme precisely. C-Terminus residues 289−311 constitute another potential hydrophobic helix that is sufficiently long to span membranes. A hydrophilic section from residues 276 to 288 with two proline residues flanks this section on the N-terminal side. Another charged proline-containing section, KPAR, flanks the hydrophobic section on its C-terminal side. The six motifs characteristic of steroid- and/or retinoid-metabolizing SDRs occur between these two sections and occupy the same relative positions in both soluble and membrane-bound SDRs (*24*). The motifs include the cofactor binding site, $G^{36}X_3GXG$, and the catalytic residues $SX_nY^{176}X_3K$. These data indicate that SDRs have a core tertiary structure, with membrane-bound SDRs having an N-terminal extension, and sometimes a C-terminal extension, for membrane interaction.

RoDH1 Is a Nonglycosylated ER Protein. We determined the subcellular locus of RoDH1 by immunofluorescence of RoDH1-transfected CHO cells. Cells were treated with Triton X-100 (which permeabilizes both plasma and internal membranes), and were analyzed by confocal laser scanning microscopy using anti-RoDH1 and fluorescein-labeled goat anti-rabbit IgG (Figure 2A). RoDH1 exhibited a signal pattern consistent with ER expression, with no indication of nuclear or plasma membrane expression. The ER was visualized by the red fluorescence of a ConA-conjugated dye (Figure 2B). In most cell types, ConA selectively binds to α-mannopyranosyl and α-glucopyranosyl residues specifically in the ER (*25*). The green fluorescence pattern of anti-RoDH1 staining was identical with the red fluorescence pattern of ConA staining; combining the two revealed yellow fluorescence, indicative of colocalization (Figure 2C). The anti-RoDH1 antibody that was used recognizes RoDH1 specifically, as shown by Western blotting of mock and RoDH1-transfected CHO cells (Figure 2D, compare lanes 1 and 2). Western blotting analysis also confirmed localization of RoDH1 with microsomes from RoDH1-transfected CHO cells (Figure 2D, lane 3) and rat liver (Figure 2D, lane 4).

Most lumenal microsomal proteins are N-glycosylated with high-mannose oligosaccharides linked to an asparagine residue in the consensus motif NX(S/T). A potential N-glycosylation site, $N^{212}VT$, exists in RoDH1. Treatment of denatured RoDH1 with endoglycosidase H, however, did not alter its molecular weight, consistent with a lack of glycosylation (Figure 2E).

N- and C-Terminal Hydrophobic Segments and Enzymatic Activity. We constructed four mutants of RoDH1 to determine the impact of the N- and C-terminal hydrophobic

```
                1                   22            41                                  66   67                  92
RoDH1           MWLYLLALVGLWNLLRFLRERKVVSHLQDKYVFITGCDSGFGNLLARQLDRRGMRVLAACLTEKGA---EQLRSKTSDRLETVILDVTKTESIVA
CRAD1           MWLYLVALVGLWTLLRFFRVRQVVSHLQDKYVFITGCDSGFGTLLARQLDRRGMRVLAACLTEKGA---EELRNKTSDRLETVILDVTKTESIVT
RDH5            MWLPLLLGALLWAVLWLLRDRQ-SLPASNAFVFITGCDSGFGRLLALQLDQKSFRVLASCLTPSGA---EDLQGVASSGFNTTLLDITDPQSFQQ
11βHSD1 MAFMKKYLLPILGLFMAYYYYSANEEFRPEMLQGKKVIVTGASKGIGREMAYHLAKMGAHVVVTARSKETLQKVVSHCLELGAASAHYIAGTMEDMTFAE
2hsd                                    MNDLSGKTVIITGGARGLGAEAARQAVAAGARVVLADVLDEEG---AATARELGDAARYQHLDVTIEEDWQR
1fmc                            MFNSDNLRLDGKCAIITGAGAGIGKEIAITFATAGASVVVSDINADAANHVVDEIQQLGGQAFACRCDITSEQELSA
1cyd                                    MKLNFSGLRALVTGAGKGIGRDTVKALHASGAKVVAVTRTN--------SD-LVSLAKECPGIEPVCVDLGD

                93                        119    120                                  157  158          173 174       185
RoDH1           ATQWVKERVGNRGLWGLVNNAGISVPV----GPNEWMRKKDFASVLDVNLLGVIEVTLNMLPLVRKARG--RVVNIASTMGRMSLVG-GGYCISKYGVEA
CRAD1           ATQWVKEHVGNRGLWGLVNNAGISTPS----GPNEWMKKQDFAHVLDVNLLGMIEVTLSMLPLVRKARG--RVVNVSSVMGRVSLFG-GGYCISKYGVEA
RDH5            AAKWVEMHVKEAGLFGLVNNAGVAGII----GPTPWLTRDDFQRVLNVNTMGPIGVTLALLPLLQQARG--RVINITSVLGRLAANG-GGYCVSKFGLEA
11βHSD1 QFVAQAGKLMG-GLDMLILNHITNTSLN----LFHD-DIHHVRKSMEVNFLSYVVLTVAALPMLKQSNG--SIVVVSSLAGKVAYPMVAAYSASKFALDG
2hsd            VVAYAREEFG--SVDGLVNNAGISTG-----MFLETESVERFRKVVDINLTGVFIGMKTVIPAMKDAGGG-SIVNISSAAGLMGLALTSSYGASKWGVRG
1fmc            LADFAISKLG--KVDILVNNAGGGGP------KPFDMPMADFRRAYELNVFSFFHLSQLVAPEMEKNGGG-VILTITSMAAENKNINMTSYASSKAAASH
1cyd            WDATEKALGGIGPVDLLVNNAALVIMQ-----PFLEVTKEAFDRSFSVNLRSVFQVSQMVARDMINRGVPGSIVNVSSMVAHVTFPNLITYSSTKGAMTM

                186                               220          221                                255 256          275
RoDH1           FSDSLRRELTYFGVKVAIIEPGGFKTNVTNMERLS---------DNLKKLWDQTTEEVKEIYGEKFQDSYMKAMESLVN-TCSGDLSLVTDCMEHALTSC
CRAD1           FSDSLRRELSYFGVKVAIIEPGFFLTGVTSSARLC---------SNTQMLWDQTSSEIREIYGEKYLASYLKRLNKLDK-RCNKDLSGVTDCMEHALTAC
RDH5            FSDSLRRDVAHFGIRESIVEPGFFRTPVTNLESLE---------KTLQACWARLPPATQAHYGGAFLTKYLKMQQRIMNLICDPDLTKVSRCLEHALTAR
11βHSD1 FFSSIRKEYSVSRVNVSITLCVLGLIDTETAMKAVSGIVHMQAAPKEECALEIIKGGALRQEEVYYDSSLWTTLLIRNP------CRKILEFLYSTSYNM
2hsd            LSKLAAVELGTDRIRVNSVHPGMTYTPMTAETGIR---------QGEGNYPNTPMGRVGNEPGE-IAGAVVKLLSDTSS------YVTGAELAVDGGWTT
1fmc            LVRNMAFDLGEKNIRVNGIAPGAILTDALKSVITP---------EIEQKMLQHTPIRRLGQPQD-IANAALFLCSPAAS------WVSGQILTVSGGGVQ
1cyd            LTKAMAMELGPHKIRVNSVNPTVVLTDMGKKVSADP--------EFARKLKERHPLRKFAEVED-VVNSILFLLSDRSAS------TSGGGILVDAGYLA

                276          289               311   317
RoDH1           HPRTRYSPGWDAKFFYLPMSYLPTFLSDAVIHWGSVKPARAL     membrane
CRAD1           HPRTRYSAGWDAKLFYLPLSYLPTFLVDALLYWTSLKPEKAL     membrane
RDH5            HPRTRYSPGWDAKLLWLPASYLPASLVDAVLTWVLPKPAQAVY    membrane
11βHSD1 DRFINK                                                 membrane
2hsd            GPTVKYVMGQ                                     soluble
1fmc            ELN                                            soluble
1cyd            S                                              soluble
```

FIGURE 1: Alignments of soluble vs membrane-bound SDR primary sequence. Protein Data Base entries were used for soluble SDRs: 2hsd (*Streptomyces* 3α,20*β*-hydroxysteroid dehydrogenase), 1fmc (*Escherichia coli* 7α-hydroxysteroid dehydrogenase), and 1cyd (mouse lung carbonyl reductase). Sequences were numbered according to RoDH1. Boldface shows the KK signal in 11*β*HSD1. Underlining denotes the sections deleted from RoDH1 and the section used from human 11*β*HSD1. The boxed areas show the six motifs characteristic of SDRs. The first motif contains the cofactor binding site. The fourth and fifth motifs contain the catalytic residues.

extensions on activity and expression loci (Figure 3). RoDH1(Δ1−18) had the first 18 N-terminal amino acids deleted. RoDH1(Δ289−317) had the last 28 C-terminal amino acids deleted. RoDH1(Δ1−18+Δ289−317) had both deletions. RoDH1(Δ289−311) had the putative C-terminal membrane region deleted, but retained the last six C-terminal mostly hydrophilic amino acids. Microsomes from CHO cells transfected with wild-type RoDH1 (15 *μ*g of protein) produced 57 ± 3.5 pmol (mean ± standard deviation of triplicate experiments) of all-*trans*-retinal from 2 *μ*M all-*trans*-retinol over the course of 10 min. Under the same conditions, microsomes from cells transfected with the mutants had only 4−7% of the activity of wild-type RoDH1. The amounts of mutants expressed in microsomes were small relative to the amount of the wild type. Therefore, enzyme assays also were done with intact cells that expressed the wild type and mutants, and with the 830*g* supernatants. The results confirmed the loss of activity in the four mutants.

N- and C-Terminal Hydrophobic Segments and Membrane Association. RoDH1 and its mutants were expressed to the same extent, as shown by Western blot analysis of the 1000*g* supernatants of transfected CHO cells (Figure 4). Relative to RoDH1 (relative distribution of 1), much less of the N-terminal deletion mutants RoDH1(Δ1−18) and RoDH1-(Δ1−18+Δ289−317) was distributed to the 10000*g* supernatant (relative distributions of <0.2 and ∼0.3, respectively). The two constructs with only C-terminal mutations, RoDH1-(Δ289−317) and RoDH1(Δ289−311), also exhibited a smaller distribution to the 10000*g* supernatant than RoDH1 (relative distributions of ∼0.5 each). Western blot analysis

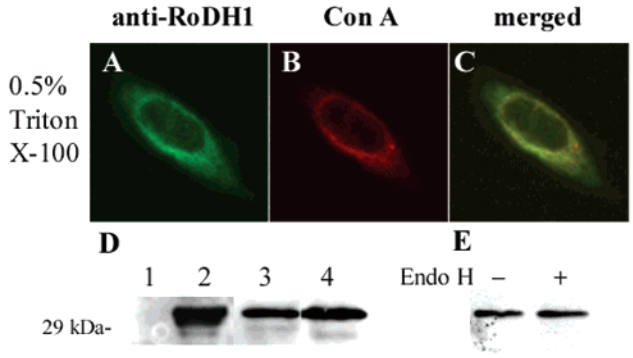

FIGURE 2: Endoplasmic reticular localization of RoDH1. CHO cells were transfected with RoDH1 and treated with anti-RoDH1. (A) Cells were incubated with fluorescein-conjugated goat anti-rabbit IgG (green). (B) The same cells also were treated with Texas red-conjugated ConA (red). (C) Merged images of panels A and B revealing localization of RoDH1 in the ER. (D) Western blot analysis with anti-RoDH1 of (lane 1) mock transfected CHO cells (10000*g* supernatant), (lane 2) RoDH1-transfected CHO cells (10000*g* supernatant), (*lane 3*) RoDH1-transfected CHO cell microsomes, and (lane 4) rat liver microsomes. (E) Endoglycosidase H treatment of microsomes solubilized from RoDH1-transfected CHO cells. Five micrograms of protein was applied in each lane, and signals were visualized by chemiluminescence.

verified the presence of expressed proteins in the 10000*g* pellets (data not shown); i.e., the changes in distribution did not represent losses during handling. Analysis of the 100000*g* pellet prepared from the 10000*g* supernatant reflected these results, showing the virtual absence of N-terminal mutants from the microsomes, but the occurrence of C-terminal

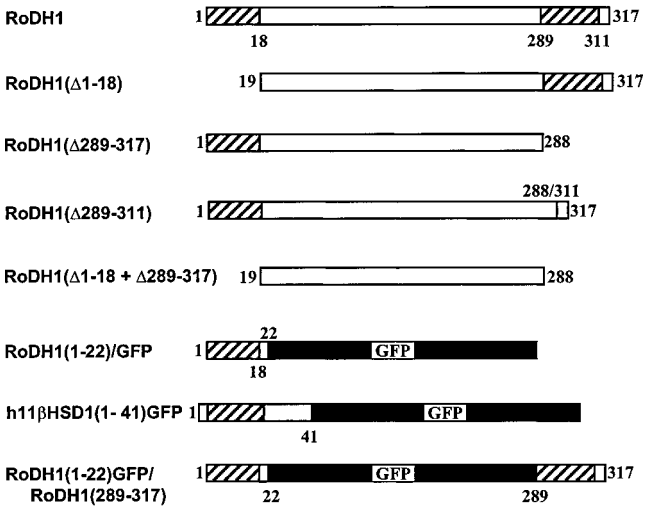

FIGURE 3: RoDH1 mutants and GFP fusion proteins. The structures of the reported constructs are shown. Striped boxes represent potential transmembrane segments. White boxes represent the remaining residues of RoDH1 or the indicated section of h11βHSD1. Black boxes represent GFP.

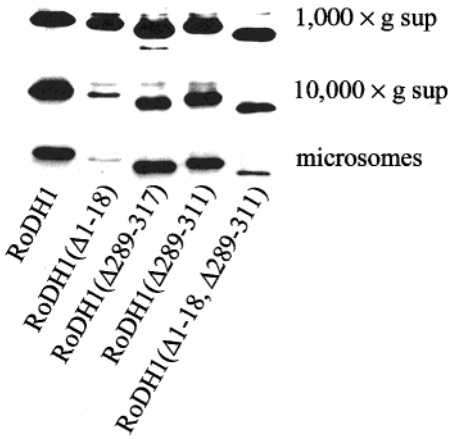

FIGURE 4: Membrane distribution of RoDH1 mutants. Western blot analysis with anti-RoDH1 of transfected CHO cell lysates: (top) 1000*g* supernatant, (middle) 10000*g* supernatant, and (bottom) 100000*g* pellet. Fifteen micrograms of protein was loaded onto each lane.

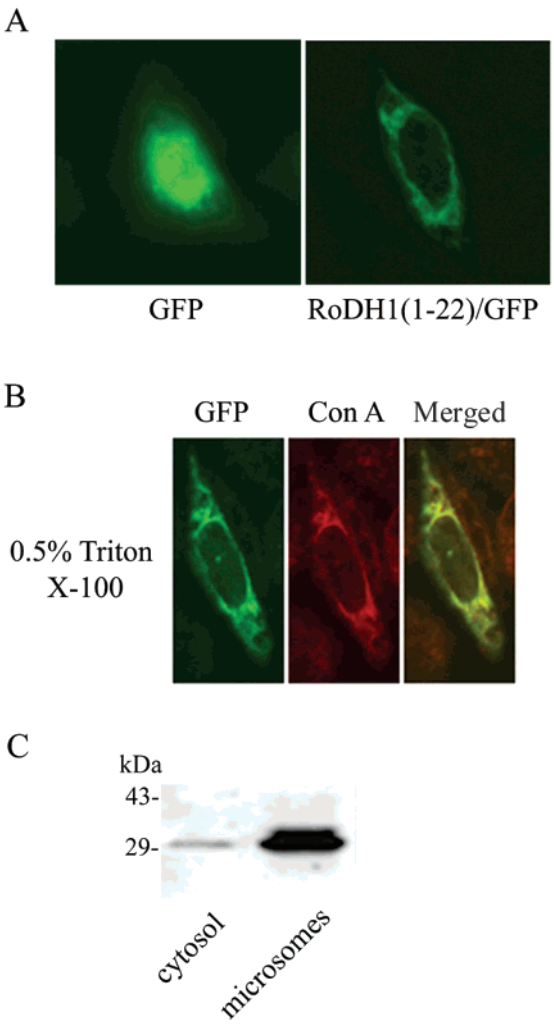

FIGURE 5: Subcellular localization of a RoDH1(1−22)−GFP fusion protein. Representative fluorescence images and Western blots are shown of CHO cells transfected with the RoDH1(1−22)−GFP protein. (A) Subcellular distribution in CHO cells. (B) Localization of the RoDH1(1−22)−GFP fusion protein in the ER membrane: left, GFP fluorescence (green); middle, staining of the ER by Texas red-conjugated ConA (red); and right, merged image of the fusion protein and ConA (yellow). (C) The 100000*g* supernatant and the microsomal pellets (10 μg of protein each) of the RoDH1(1−22)−GFP protein expressing CHO cells were analyzed by Western blot analysis.

mutants in the microsomes. These results indicate that the N-terminal hydrophobic region targets RoDH1 to the microsomes, the lack of the C-terminal hydrophobic region reduces, but does not preclude, RoDH1 association with microsomes, and RoDH1 lacking both regions still associates with membranes, but not well with microsomal membranes.

The N-Terminus of RoDH1 Is a Transmembrane Region That Is Sufficient for ER Targeting. To confirm the function of the N-terminal hydrophobic region, the RoDH1(1−22)−GFP fusion protein was constructed with the first 22 amino acid residues of RoDH1 fused to the N-terminus of the soluble GFP. The RoDH1(1−22)−GFP fusion protein had a typical membrane localization pattern, whereas native GFP had a diffuse and distinct pattern (Figure 5A). To confirm that the fluorescence distribution along the reticular network characterizes ER localization, we compared the green fluorescence pattern of the RoDH1(1−22)−GFP protein (Figure 5B, left) with a ConA staining pattern, indicated by red fluorescence (Figure 5B, middle). The yellow signal produced by combining the green and red fluorescence signals revealed localization of the RoDH1(1−22)−GFP fusion protein in the ER (Figure 5B, right). Western blotting also indicated microsomal localization of the RoDH1(1−22)−GFP protein (Figure 5C). These results corroborate the function of the first N-terminal amino acids of RoDH1 in ER targeting and membrane anchoring.

RoDH1 Faces the Cytosol. Proteinase K protection assays were done to determine the orientation of RoDH1. At 4 °C, RoDH1 resisted proteinase K digestion in both the absence and presence of 1% Triton X-100 (Figure 6A, top left). Under the same conditions, the lumenal-orienting signal peptide of an SDR with steroid dehydrogenase activity attached to GFP resulted in a fusion protein, 11βHSD1(1−41)−GFP, that was protected from proteinase K digestion only in the absence of Triton X-100 (Figure 6A). These results suggested that RoDH1 resists proteinase K action at low temperatures. At 37 °C, however, proteinase K degraded RoDH1 in the absence and presence of Triton X-100 (Figure 6A). In

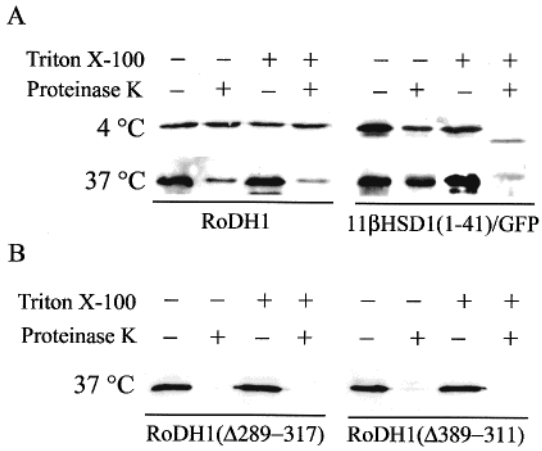

FIGURE 6: Proteinase K protection assays with RoDH1 and its mutants. Western blot analysis of protease K digestion (50 μg/mL) of transfected CHO cell microsomes in the absence or presence of 1% Triton X-100. (A) Proteinase K digestion of RoDH1 and h11βHSD1(1−41)−GFP. (B) Proteinase K digestion of RoDH1-(Δ289−317) and RoDH1(Δ289−311).

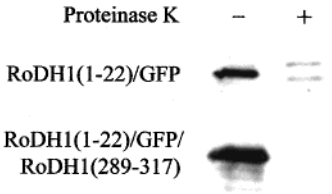

FIGURE 7: Proteinase K assays of RoDH1(1−22)−GFP and RoDH1−GFP−RoDH1(Δ289−317) fusion proteins. Fusion proteins (5 μg of microsomal protein from transfected CHO cell lysates) were treated with proteinase K at 37 °C for 2 h.

contrast, at 37 °C the lumenal-facing 11βHSD1(1−41)−GFP fusion protein was degraded by proteinase K only in the presence of Triton X-100 (Figure 6A, right). Clearly, RoDH1 behaves differently with respect to proteinase K digestion from a fusion protein made with an SDR signal sequence established as a lumenal-facing anchor.

Proteinase K protection assays with the mutants RoDH1-(Δ289−317) and RoDH1(Δ289−311) showed that both were degraded in the absence of Triton X-100 somewhat more thoroughly than native RoDH1 (Figure 6B). This indicated that these mutants were oriented toward the cytosol, accessible to the protease. Proteinase K protection assays also revealed that the RoDH1(1−22)−GFP fusion protein faces the cytosol (Figure 7). To further test whether C-terminal hydrophobic residues 289−317 affect the orientation of RoDH1, a fusion protein was constructed with GFP situated between both extensions of RoDH1, i.e., RoDH1(1−22)−GFP−RoDH1(Δ289−317) (Figure 1). The proteinase K protection assay of the RoDH1(1−22)−GFP−RoDH1-(Δ289−317) that remained within the glycerol-extracted microsomes (i.e., with peripheral membrane proteins extracted and only tightly associated members remaining) showed proteinase K sensitivity in the absence of Triton X-100, indicating exposure to cytosol. This eliminated the possibility that residues 289−317 signal lumenal orientation of RoDH1.

DISCUSSION

At least 15 structures of soluble SDRs have been determined by X-ray crystallography (*27*, *28*). Despite levels of amino acid identity as low as 15%, these soluble SDRs share strikingly similar globular structures and substrate access portals (*24*, *28*). The 255-amino acid cores of both soluble and membrane-associated SDRs share the same six characteristic SDR motifs, including the same arrangements of conserved amino acids that form cofactor binding sites, catalytic residues, and secondary structure. The primary structures of membrane-bound SDRs differ from soluble SDRs predominantly in the former having a hydrophobic extension beyond the shared core at the N-termini and sometimes at the C-termini. These insights and our data are consistent with RoDH1 folding into an ER-associated globular protein that faces the cytosol and uses the C-terminal segment to enhance ER association and protein stability and/or optimum folding. A model consistent with these insights allows a cytosol-facing RoDH1 with the N-terminus anchored in the membrane and the C-terminal hydrophobic segment extending along the membrane (Figure 8). Such a membrane association pattern has been postulated for prostaglandin endoperoxide H synthases 1 and 2 (*29*).

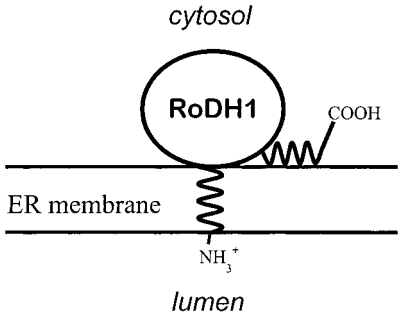

FIGURE 8: Proposed association of RoDH1 with microsomal membranes. The N-terminal hydrophobic region directs RoDH1 to the microsomal membrane and anchors the protein, but does not cause it to enter the lumen. The C-terminal hydrophobic region may help associate RoDH with membranes, but does not cause RoDH1 to pass through the membrane to face the lumen. Thus, RoDH1 orients itself toward the cytosol. The degree to which RoDH1 embeds in the membrane remains uncertain. The depiction of it sitting on top of the membrane does not preclude the possibility that the globular structure of RoDH1 might penetrate partially into the membrane bilayer.

The low enzymatic activity of mutants truncated at the N- or C-terminal ends might have different causes. A model of protein insertion into the endoplasmic reticulum has the N-terminal signal sequence associate with the aqueous channel formed in the membrane from the heterotrimeric Sec61p complex as the remaining protein undergoes translation (*38*). The ribosome remains membrane-bound during protein synthesis, and transmembrane domains can leave the channel laterally during translation. An enzyme lacking the N-terminal signal sequence would not associate with the channel, and may not fold properly. On the other hand, according to this model, a protein lacking its membrane-associated C-terminus should fold properly to a point, but may not associate properly with the membrane: both incomplete folding and a decreased level of membrane association could cause loss of activity.

The model (Figure 8) allows for facile recognition of cytosolic holo-CRBP as a substrate by microsomal RoDH1 (*7*). Evidence supporting a substrate function for holo-CRBP during RA biosynthesis includes kinetic experiments that distinguish between holo-CRBP and unbound

retinol as substrates. Briefly, increasing the concentrations of holo-CRBP, while maintaining a constant concentration of unbound retinol, provides Michaelis−Menten kinetics for the rate of retinal formation. Alternatively, maintaining a constant holo-CRBP concentration while decreasing the concentration of free retinol does not alter the rate of retinal production, until the apo-CRBP:holo-CRBP ratio exceeds 1:1. Both specify access of microsomal RoDH to retinol bound with CRBP. Moreover, holo-CRBP, but not apo-CRBP, cross-links with semipurified RoDH and RoDH in rat liver microsomes only in the presence of cofactor, as expected for the ordered bisubstrate reaction characteristic of dehydrogenases (*8*). Cross-linking appears to be specific because in microsomes, a milieu replete with multiple enzymes, only RoDH and LRAT bind covalently with derivatized CRBP. Mutation of a single exterior residue of CRBP, not involved in protein folding or ligand binding, i.e., L35A, produced retinal with a V_m decreased relative to that of wild-type CRBP, without an apparent change in K_d or folding, suggesting that the protruding L35 mediates interaction between CRBP and RoDH (*30*). Finally, a RA-generating system has been reconstituted from holo-CRBP, microsomes, and purified retinal dehydrogenases, verifying the function of the major physiological form of retinol, holo-CRBP, as a substrate provider (*31*, *32*).

Various arguments can be made for predicting the directionality of retinoid/steroid dehydrogenase-catalyzed reversible reactions. One would rely on the high NAD^+:NADH and NADPH:$NADP^+$ ratios in liver to drive NAD^+-dependent dehydrogenases in the oxidative direction and $NADP^+$-dependent dehydrogenases in the reductive direction (*33*). Another would rely on the oxidative environment of the ER lumen, compared to the reductive environment of cytosol, to house oxidative SDR (*34*). The directionality of metabolic enzymes often does not yield to such analyses. For example, h11βHSD1 represents a NADPH-dependent, lumenal-facing SDR that functions in both directions, but is primarily reductive in vivo (*35*). h11βHSD2 represents an NAD^+-dependent, cytosolic-facing SDR that functions oxidatively (*36*). RoDH1 can use either $NADP^+$ or NAD^+ in vitro, and functions in the oxidative direction when assayed in intact cells.[2] Thus, despite the relatively reductive environment of cytosol, RoDH1 as well as h11βHSD2, and a host of other cytosol-exposed dehydrogenases, function oxidatively.

Mouse CRAD1 has been proposed as a lumenal-facing ER-associated SDR, based on a slower rate of proteinase K digestion at 4 °C in the absence of Triton X-100 relative to that in its presence (*37*). The sequences of mouse CRAD1 and rat RoDH1 are 86% similar overall, and 90% similar in the two hydrophobic extensions that consist of amino acid residues 1−22 and 289−317. These two proteins likely fold and orient similarly. Slow digestion of CRAD1 by proteinase K at 4 °C resembles RoDH1 resistance, and contrasts with the stability of the lumenal-facing h11βHSD1−GFP protein in the absence of detergent, even at 37 °C. The CRAD1 data and the similarities between CRAD1 and RoDH1 seem more indicative of CRAD1 facing the cytosol. Consistent with this conclusion, neither CRAD1 nor RoDH1 has the N-terminal di-lysine or di-arginine residues responsible for the lumenal orientation of 11βHSD1 (*18*, *19*).

[2] J. Wang and J. L. Napoli, unpublished data.

In summary, this report shows that the N-terminus of RoDH1, a prototypical retinoid/steroid-metabolizing SDR, provides a necessary and sufficient signal for anchoring the enzyme to the ER oriented toward the cytosol. Removal of the C-terminus reduces but does not prevent ER association. Removal of both the N- and C-termini eliminates ER association, but does not generate a soluble protein, suggesting that the SDR core of RoDH1 has overall external hydrophobicity.

REFERENCES

1. Moore, T. M. (1957) *Vitamin A*, Elsevier, New York.
2. Wolf, G. (1984) *Physiol. Rev. 64*, 674−937.
3. Sucov, H. M., and Evans, R. M. (1995) *Mol. Neurobiol. 10*, 169−184.
4. Chambon, P. (1996) *FASEB J. 10*, 940−954.
5. Napoli, J. L. (2000) *Prog. Nucleic Acid Res. Mol. Biol. 63*, 139−188.
6. Duester, G. (1996) *Biochemistry 35*, 12221−12227.
7. Posch, K. C., Boerman, M. H. E. M., Burns, R. D., and Napoli, J. L. (1991) *Biochemistry 30*, 6224−6230.
8. Boerman, M. H. E. M., and Napoli, J. L. (1995) *Biochemistry 34*, 7027−7037.
9. Ottonello, S., Scita, G., Mantovani, G., Cavazzini, D., and Rossi, G. L. (1993) *J. Biol. Chem. 268*, 27133−27142.
10. Kedishvili, N. Y., Gough, W. H., Davis, W. I., Parsons, S., Li, T. K., and Bosron, W. F. (1998) *Biochem. Biophys. Res. Commun. 249*, 191−196.
11. Rong, D., Lin, C. L., d'Avignon, D. A., Lovey, A. J., Rosenberger, M., and Li, E. (1997) *FEBS Lett. 402*, 116−120.
12. Chai, X., Boerman, M. H. E. M., Zhai, Y., and Napoli, J. L. (1995) *J. Biol. Chem. 270*, 3900−3904.
13. Blobel, G. (1980) *Proc. Natl. Acad. Sci. U.S.A. 77*, 1496−1500.
14. Munro, S., and Pelham, H. R. (1987) *Cell 46*, 291−300.
15. Scheel, A. A., and Pelham, H. R. (1996) *Biochemistry 35*, 10203−10209.
16. Ozols, J. (1995) *J. Biol. Chem. 270*, 2305−2312.
17. Simon, A., Romert, A., Gustafson, A.-L., MaCaffery, M., and Eriksson, U. (1999) *J. Cell Sci. 112*, 549−558.
18. Odermatt, A., Arnold, P., Stauffer, A., Frey, B. M., and Frey, F. J. (1999) *J. Biol. Chem. 274*, 28762−28770.
19. Mziau, H., Korza, G., Hand, A. R., Gerard, C., and Ozols, J. (1999) *J. Biol. Chem. 274*, 14122−14129.
20. Romert, A., Tuvendal, P., Tryggvason, K., Dencker, L., and Eriksson, E. (2000) *Exp. Cell Res. 256*, 338−345.
21. Chai, X., Zhai, Y., and Napoli, J. L. (1997) *J. Biol. Chem. 272*, 33125−33131.
22. Su, J., Chai, X., and Napoli, J. L. (1998) *J. Biol. Chem. 273*, 17910−17916.
23. Jörnvall, H., Persson, B., Krook, M., Atrian, S., Gonzàlez-Durate, R., Jeffry, J., and Ghosh, D. (1995) *Biochemistry 34*, 6003−6013.
24. Bailey, T. L., Baker, M. E., and Elkan, C. P. (1997) *J. Steroid Biochem. Mol. Biol. 62*, 29−44.
25. Spector, D. L., Goldman, R. D., and Leinwood, L. A. (1998) *Cells: a Laboratory Manual*, Cold Spring Harbor Laboratory Press, Plainview, NY.
26. Benach, J., Atrian, S., Gonzàlez-Duarte, R., and Ladenstein, R. (1998) *J. Mol. Biol. 282*, 383−399.
27. Grimm, C., Maser, E., Möbus, E., Klebe, G., Reuter, K., and Ficner, R. (2000) *J. Biol. Chem. 275*, 41333−41339.
28. Duax, W. L., Ghosh, D., and Pletnev, V. (2000) *Vitam. Horm. 58*, 121−148.
29. Spencer, A. G., Thuresson, E., Otto, J. C., Song, I., Smith, T., Dewitt, D. L., Garavito, R. M., and Smith, W. L. (1999) *J. Biol. Chem. 272*, 32936−32942.
30. Penzes, P., and Napoli, J. L. (1999) *Biochemistry 38*, 2088−2093.
31. Posch, K. C., Burns, R. D., and Napoli, J. L. (1992) *J. Biol. Chem. 267*, 19676−19682.

32. Wang, X., Penzes, P., and Napoli, J. L. (1996) *J. Biol. Chem. 271*, 16288−16293.
33. Veech, R. L., Eggleston, L. V., and Krebs, H. A. (1969) *Biochem. J. 115*, 609−619.
34. Hwang, C., Sinskey, A. J., and Lodish, H. F. (1992) *Science 257*, 1496−1502.
35. Stewart, P. M., and Krozowski, Z. S. (1999) *Vitam. Horm. 57*, 249−324.
36. White, P. C., Mune, T., and Agarwal, A. K. (1997) *Endocr. Rev. 18*, 135−156.
37. Tryggvason, K., Romert, A., and Eriksson, U. (2001) *J. Biol. Chem. 276* (in press).
38. Mothes, W., Heinrich, S. U., Graf, R., Nilsson, I., von Heijne, G., Brunner, J., and Rappoport, T. A. (1997) *Cell 89*, 523−533.

BI011396+